Chemistry Faculty Research & Creative Works   Chemistry

15 Sep 2022

Laboratory Evaluation of a Novel Self-Healable Polymer Gel for CO2 Leakage Remediation during CO2 Storage and CO2 Flooding

Tao Song

Zhanmiao Zhai

Junchen Liu

Yugandhara Eriyagama

et. al. For a complete list of authors, see *https://scholarsmine.mst.edu/chem_facwork/3172*

Recommended Citation

Laboratory evaluation of a novel Self-healable polymer gel for CO_2 leakage remediation during CO_2 storage and CO_2 flooding

Tao Song [a], Zhanmiao Zhai [a], Junchen Liu [a], Yugandhara Eriyagama [b], Mohamed Ahdaya [a], Adel Alotibi [a], Ze Wang [a], Thomas Schuman [b], Baojun Bai [a,*]

[a] Department of Geosciences and Geological and Petroleum Engineering, Missouri University of Science and Technology, Rolla, MO 65409, USA
[b] Department of Chemistry, Missouri University of Science and Technology, Rolla, MO 65409, USA

A R T I C L E I N F O

A B S T R A C T

For CO_2 storage in subsurface reservoirs, one of the most crucial requirements is the ability to remediate the leakage caused by the natural fractures or newly generated fractures due to the increasing pore pressure associated with CO_2 injection. For CO_2 Enhanced Oil Recovery (EOR), high conductivity features such as fractures and void space conduits can severely restrict the CO_2 sweep efficiency. Polymer gels have been developed to plug the leakage and improve the sweep efficiency. This work evaluated a CO_2 resistant branched self-healable preformed particle gel (CO_2-BRPPG) for CO_2 plugging purpose. This novel CO_2-BRPPG can reform a mechanical robust adhesive bulk gel after being placed in the reservoir and efficiently seal fractures. In this work, the swelling kinetics, self-healing behavior, thermal stability, CO_2 stability, rheology, adhesion property and plugging performance of this novel CO_2-BRPPG were studied in the laboratory. Results showed that this CO_2-BRPPG has good self-healing abilities, and the self-healed bulk gel has excellent mechanical and adhesion strength. Gel with a swelling ratio of ten has an elastic modulus of over 2000 Pa, and the adhesion strength to sandstone is 1.16 psi. The CO_2-BRPPG has good CO_2 phase stability at 65 °C, and no dehydration was observed after 60 days of exposure to 2900 psi CO_2 at 65 °C. Core flooding test proved that the swelled particles could reform a bulk gel after being placed in the fractures, and the reformed bulky gel has excellent CO_2 plugging efficiency. The supercritical CO_2 breakthrough pressure gradient was 265 psi/feet (5.48 MPa/m). This work could offer the experimental basis for the field application of this CO_2-BRPPG in CO_2 storage and CO_2 enhanced oil recovery.

1. Introduction

Global climate change caused by anthropogenic carbon dioxide emission is one of the main challenges faced by industrial countries. Several methods have been developed to address the significant increase in CO_2 emissions, such as CO_2 capture and sequestration, where CO_2 was safely stored in saline aquifers, depleted oil and gas reservoirs or other underground geological formations with adequate pore space, good connectivity, and impermeable caprock [1–9]. Among all these methods, CO_2 sequestration in depleted oil and gas reservoirs was considered the most efficient and economical method because the reservoirs' geological and petrophysical properties have been well diagnosed during the drilling and production process [7,10–12]. In addition, the CO_2 enhanced oil recovery is highly valued in the petroleum industry due to its low cost, high efficiency in oil recovery improvement, and broad applicability [7,10]. It was estimated that during the CO_2

EOR process, 3 kg of CO_2 could be sequestrated with 1 kg of oil being produced [13].

However, the high conductivity features are a significant challenge that threatens CO_2 sequestration and CO_2 flooding. The existence of high conductivity features such as natural fractures and void space conduits could substantially deteriorate the CO_2 sequestration and flooding efficiency [1,14]. CO_2 could flow or leak through these high conductivity features and result in early and excessive CO_2 production and unsuccessful sequestration treatment. Polymer gel treatment as a cost-effective method has been deployed in the oil industry to reduce excessive water or gas production and improve oil recovery [15]. In situ gel and preformed particle gels (PPG) are two types of gel systems that are commonly used in fields. The in-situ gel treatment involves simultaneous or sequential polymer and crosslinker solution injection. The polymer and crosslinker solution can change to gel under reservoir conditions, physically diverting the post-injected water or gas [16]. The

in-situ gel systems have good performance in blocking high permeability matrix and tiny fractures [17,18]. Martin reported that the gel composed of 3.6% of polymer and 0.07% of dichromate, 0.21% of sodium thiosulfate has a CO_2 plugging efficiency of 84.1% in the first cycle of CO_2 flooding at 40.6 °C under 1500 psi [19]. Seright reported that a gel system composed of 1.39% of polymer and 0.0212% of Cr (III) could efficiently decrease CO_2 permeability in the first cycle of CO_2 injection. However, the plugging efficiency gradually decreased with the increase of water alternative gas (WAG) cycles. The plugging efficiency under 900 psi of CO_2 in the first, second and third cycles of WAG was 99.98, 99.8 and 92.8%, respectively [15]. Taabbodi evaluated two kinds of Cr (III)-based gel systems, one is 0.72% of high molecular weight polymer and 0.03% of Cr (III), and the other is 5% low molecular weight polymer and 0.42% of Cr (III) at 40 °C under 1200 psi. Results showed that both gel systems could reduce the CO_2 permeability to over 100 times, and the CO_2 plugging efficiency can reach up to 99.7% at 40 °C under 1200 psi [20]. Preformed particle gels (PPG), a kind of superabsorbent polymers, are gel particles prepared at a surface facility. They can swell a few to several hundred of their original volume in brine. PPG can be selectively placed in fractures due to the controllable particle size and deformable characteristics. It can significantly enhance the conformance of fractured reservoirs by filling and blocking off the high conductivity paths [21–23]. However, only a few publications have reported the application of PPG in CO_2 flooding projects. For example, One field application in the Cowden Unit in Texas showed that the PPG could plug the high permeability thief zone for five months [24]. Ze et al. reported the application of CO_2 responsive PPG in plugging open fractures [25]. This water-swellable CO_2 responsive PPG could further swell by approximately two times in supercritical CO_2 conditions, and the CO_2 breakthrough pressure can reach up to 437.2 psi.

However, for reservoirs with large fractures or void space conduits, the effectiveness of in-situ gel and PPGs is usually very limited [26–28]. David Smith mentioned that the early field application in Anton Irish Clearfork proved that the in-situ gel could not alleviate the excessive CO_2 production due to the existence of void space conduits and the low mechanical strength of the HPAM/Cr (III) gel [27]. The final gel strength can be enhanced by increasing the polymer and crosslinker concentration, but the maximum polymer concentration is usually below 10%. This is because the injection pressure increases exponentially with polymer concentrations, raising injectivity issues. Too high injection pressure might generate new fractures at the near-wellbore regions, further aggravating the reservoir heterogeneity. Furthermore, the crosslinked gel has a half-decent long-term thermal and phase stability under CO_2 conditions in matrix plugging treatment, where the in-situ gel has a limited contact area with CO_2 [29]. However, the stability of the in-situ gels decreases precipitously with the increase of gel and CO_2 contact areas, which makes it a poor candidate for CO_2 plugging in fractured reservoirs, where the polymer gel is directly exposed to CO_2 [30]. In the case of PPG treatment, field application in the West Sak field of Alaska proved PPG's inability to treat reservoirs with void space conduits [26]. The gel particles were found in the production separators, indicating that the PPG was produced from the void space conduits over time because of the lack of particle–particle association and particle rock adhesion. In addition, the particle–particle and particle-rock interfaces could act like tiny fractures to water and gas if the gel particles were not well packed. Furthermore, traditional PPG products are crosslinked polyacrylamide, which is unstable under CO_2 or supercritical CO_2 conditions, and severe dehydration can be observed after long-term CO_2 exposure [31]. The failure mechanism was attributed to the low pH condition created by the CO_2 [32,33].

Our group has recently developed a new CO_2-resistant hyperbranched self-healable PPG (CO_2-BRPPG) composed of a high concentration of CO_2-resistant monomers. This novel CO_2-BRPPG can swell in brine solutions and self-healing to form a robust adhesive bulk gel. The bulk gel could adhere to the fractures or void space conduits and be stable in CO_2 and supercritical CO_2 conditions. In this paper, we systematically evaluated this CO_2-BRPPG. First, the effect of salinity and pH on the swelling kinetics of CO_2-BRPPG was studied. Then, the gel strength, tensile and adhesion properties of the CO_2-BRPPG to sandstone and carbonate were evaluated. Third, the thermal stability and CO_2 stability of the CO_2-BRPPG were assessed by monitoring strength changes of the self-healed gels at 65 °C. Besides, a fractured sandstone model was employed to test the plugging efficiency of the CO_2-BRPPG to supercritical CO_2.

2. Experimental section

2.1. Materials and a brief description of the CO_2-BRPPG

All chemicals and reagents were purchased from Sigma-Aldrich (St. Louis, MO) except as noted. Acrylamide (AM), Ammonium cerium(IV) nitrate (CAN), Zirconium acetate solution (16%), L-lysine monohydrochloride (Lys-HCl), N,N′-Methylenebisacrylamide (MBA) were used as received. 2-acrylamido-2-methylpropanesulfonic acid (AMPS) was neutralized to generate AMPS-Na before using. The AMPS-Na preparation method was listed in the previous work [29]. The CO_2-BRPPG commercial product provided by Daqing Xinwantong Company was used as received without further purification. Cylindrical Berea Sandstone core was used for the core flooding test. As shown in Fig. 1, the swelled gel has excellent self-healing properties. The two bulk gels can re-form a bulk gel after curing for four days at ambient temperatures.

2.2. Hydrogel synthesis

CO_2-BRPPG hydrogels were prepared by aqueous free-radical polymerization, as shown in Fig. 2. A typical synthesis procedure is as follows: AMPS-Na (12.17 g, 53.14 mmol), AM (34.00 g, 478.87 mmol), MBA (0.003 g, 0.019 mmol), Lys-HCl (0.6 g, 3.28 mmol), and Zirconium acetate solution (15 g) were dissolved in DI water (105 g). The solution pH was adjusted to 3.5 with dilute nitric acid. The solution was transferred into a kettle reactor and sparged with Argon for 30 min before adding initiators. The polymerization was triggered by adding CAN (0.3 g, 0.55 mmol), and the reaction was continued for 48 h at ambient temperature. The resulting bulk gel was cut into cubes, dried at 65 °C and crushed into particles.

Spectroscopic analysis was carried out on the CO_2-BRPPG. The gel sample was freeze-dried before measurement. Fourier transform infrared spectroscopy (FT-IR) spectra was recorded between 4000 and 400 cm^{-1} using Nicolet iS50 FT-IR spectrometer (Thermo Fischer Scientific).

2.3. Swelling kinetics

The dynamic swelling kinetics was evaluated by immersing the gel particles into different brines. A vibrating shaker was used to simulate the dynamic swelling process. The volume of CO_2-BRPPG was recorded periodically. In addition, the effect of salinity and pH on the swelling kinetics was studied. The swelling ratio was calculated using equation (1), where V_t is the volume of CO_2-BRPPG at different time, M_o is the weight of the dried CO_2-BRPPG.

$$SR = V_t/M_o \tag{1}$$

2.4. Self-healing test

The effect of salinity and swelling ratio on the self-healing time was studied. The precise evaluation methods were listed in our previous work [34]. The beginning time was when a weak association occurred between different particles, and the ending time was when the gel strength did not increase with time.
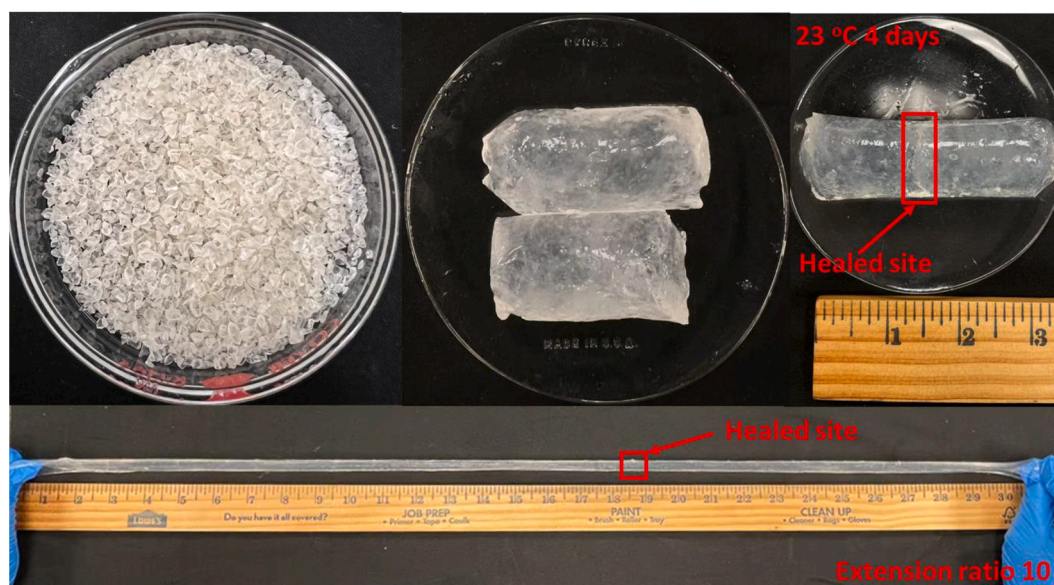
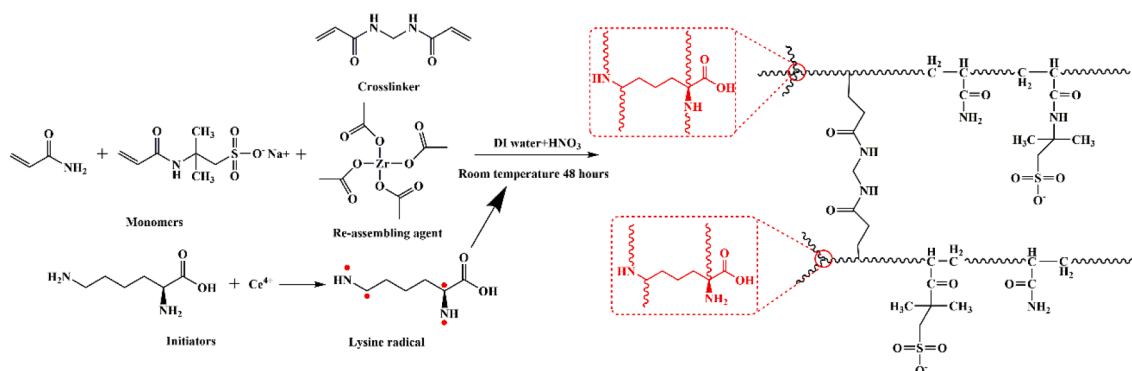**Fig. 1.** Self-healing behavior of the CO_2-BRPPG.

Fig. 2. General synthetic scheme for CO_2-BRPPG hydrogel synthesis.

2.5. Rheological, tensile and adhesion test

The rheological properties of the CO_2-BRPPG were tested using the Haake MARS III rheometer (Thermo Scientific Inc.). The spindle used in this process was P35Ti L, and the gap was set at 1 mm. The test was selected as the oscillation time-dependent experiments model with a fixed frequency of 1 Hz and a controlled strain of 1% to obtain elastic modulus (G') and viscous modulus (G''). G' was used to evaluate the strength of the gel.

All the tensile stress–strain measurements were performed on an Instron 3400 (max load 5 kN). Samples were cut into rectangular sheets (25*15*5 mm). The loading rate of the tensile test was 100 mm/min. The adhesion strength between rock and gel was studied by testing the detaching strength. A hook was glued at one side of the rock using epoxy glue, and the other side was attached to the self-healed CO_2-BRPPG. A spring scale was used to test the detach force after four days of curing at 45 °C, and the adhesion strength was calculated using equation (2), where F (N) is the maximum strength during the detach test, A (m^2) is the interaction area between gels and rock.

$$P_{adhesion} = \frac{F}{A} \tag{2}$$

2.6. Thermal and CO$_2$ stability evaluations

The long-term thermal stability evaluation was carried out using

ampoules. After adding the gel slurry into the ampoule, argon was purged into the slurry to remove oxygen for 20 min before sealing. The volume of the gel was monitored during the long-term thermal stability test. High temperature and high-pressure stainless-steel vessels were deployed to evaluate the CO_2 stability of the CO_2-BRPPG. A pump and an accumulator were employed to fill the vessel with CO_2. A typical CO_2 exposure experiment is as follows: 15.0 g of fully reassembled gel was placed in the vessel. Then the vessel was connected to an accumulator pre-filled with CO_2 (1300 psi). After that, we use a pump to transfer the CO_2 from the accumulator to the vessel till the vessel pressure reachs 1300 psi. Next, we seal the vessel, stop the pump, and put the vessel in a pre-heated 65 °C oven. After 12 h of aging, we release some CO_2 to let the pressure drop to 2900 psi.

2.7. Core flooding test

Core flooding experiments were carried out to test the plugging efficiency of this novel CO_2-BRPPG to supercritical CO_2. A round sandstone core was cut through the center to create an artificial fracture, and two stainless-steel strips were used to support the fracture. The core was precoated with epoxy glue to prevent the CO_2-BRPPG from penetrating into the matrix. The parameters of the core and experiment setup are shown in Fig. 3.

The CO_2-BRPPG injection and supercritical CO_2 flooding were performed with a system pressure of 1100 psi, and a backpressure regulator
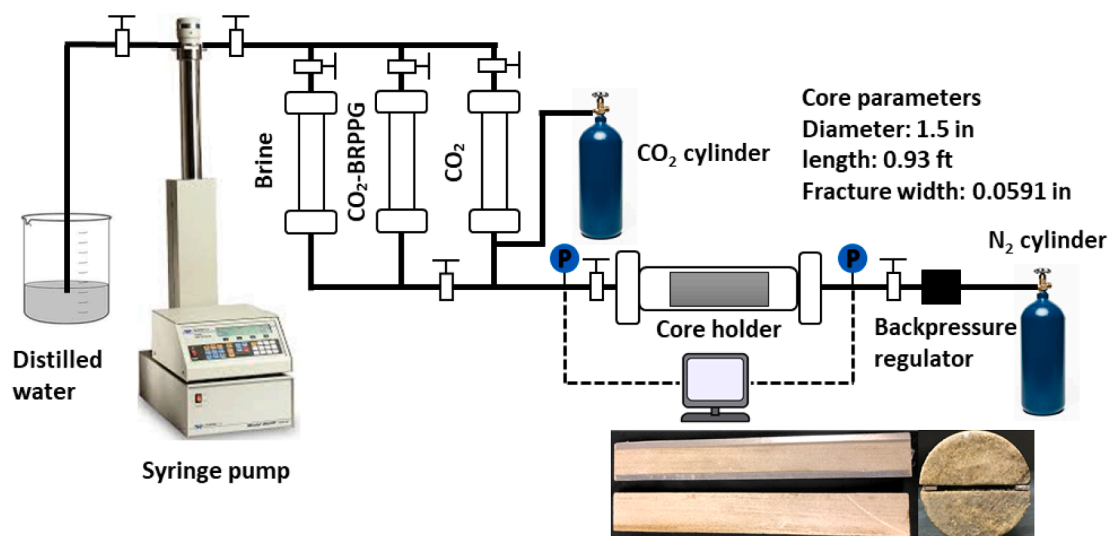
Fig. 3. Schematic of core flooding setup.

was employed to maintain the system pressure. The experiment procedure is as follows. First, the dried gel particle was swelled in 1% NaCl. Then, the gel particle slurry was placed in the fracture with an injection rate of 0.5 mL/min. After that, the core was aged at 45 °C for four days to cure the gel slurry fully. Next, a stepwise breakthrough test was performed to test the breakthrough pressure using supercritical CO_2. The breakthrough pressure was the pressure when the first drop of fluid came out of the core outlet. Finally, after breakthrough, the injection rate was sequentially changed to different flow rates and the stable pressure for each flow rate was recorded to calculate the residual resistance factor, F_{rr}, using the following equation 3–5.

$$F_{rr} = \frac{k_{initial}}{k_{after}} \tag{3}$$

$$k_{initial} = \frac{h^2}{12} \tag{4}$$

$$k_{after} = \frac{q \times \mu \times L}{A \times \Delta P} \tag{5}$$

Where $k_{initial}$ is the initial permeability of the fracture and k_{after} is the fracture permeability after gel treatment. $k_{initial}$ and k_{after} were calculated using the above equations, h is the height of the fracture (μm), q is the flow rate (cm³/s), μ is the viscosity of the liquid (cp), L is the length of the core (cm), A is the cross-sectional area (cm²) of the fracture, and ΔP is the pressure change (atm).

The self-healing property of the CO_2-BRPPG was studied by pushing the bulky gel through a slotted disk model. The experiment setup is shown in Fig. 4. The bulky gel was compressed by a piston with different pressure, and the self-healing behavior and dehydration volume were recorded.

3. Results and discussion

3.1. CO₂-BRPPG preparation

The CO_2-BRPPG is a crosslinked branched poly AM-co-AMPS, which can re-crosslink/re-assemble through the association between the polymer chains and the pre-embedded Zr (IV). Fig. 5 shows the FT-IR of the CO_2-BRPPG. The peaks around 3190 and 3334 cm⁻¹ are identified as the absorption band of amine groups from AM, AMPS and Lys-HCl. The peaks around 1186 and 1041 cm⁻¹ are assigned to the absorption band of sulfonic groups.

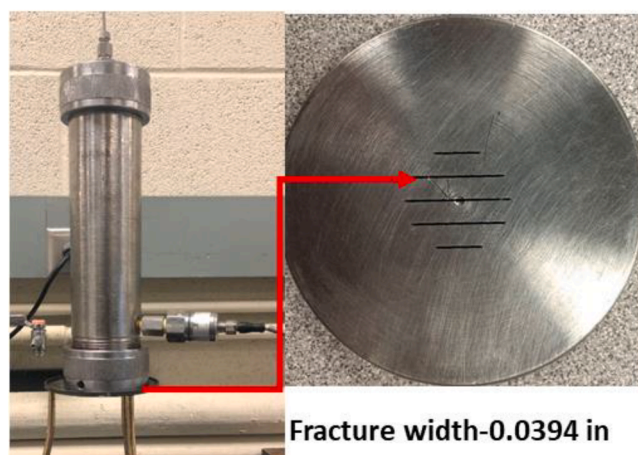The CO_2 resistance was achieved by introducing anionic monomer

Fig. 4. Schematic of breakthrough experiment setup.

AMPS, which is insensitive to the acidic condition created by the CO_2. Both field and lab tests have proved the poor stability of PAM and HPAM under CO_2 conditions, and the addition of AMPS could improve the gels' stability under CO_2 conditions [30,33,35]. The self-healing ability was attributed to the association between the pre-embedded Zr (IV) ions and polymer chains. Several ions such as B, Fe, Co, Al, Cr, and Zr have been applied to generate self-healing materials [36–39]. These ions could interact with the polymer chains through electrostatic attraction and endow the polymer gels with self-healing ability.

3.2. Swelling kinetics

CO_2-BRPPG dry particles with the size of 2–4 mm were used for the swelling kinetic evaluations. The swelling kinetic assessment was conducted in NaCl and $CaCl_2$ brine solutions and simulated Oman seawater. Fig. 6 (a) demonstrates the effect of salinity on the swelling kinetic and equilibrium swelling ratio. The CO_2-BRPPG took around 5 h to reach the equilibrium swelling ratio. The equilibrium swelling ratio in 1% NaCl, 1% $CaCl_2$ and Oman seawater (Total dissolved solid 42280 mg/L, Ca^{2+} and Mg^{2+}, 1902 mg/L) were 42, 35 and 34, respectively. The swelling rate of a polymer gel is mainly affected by the osmatic pressure and elastic retractive force applied to the polymer network [40]. The osmotic pressure decreases as the number of ions diffuse into the polymer
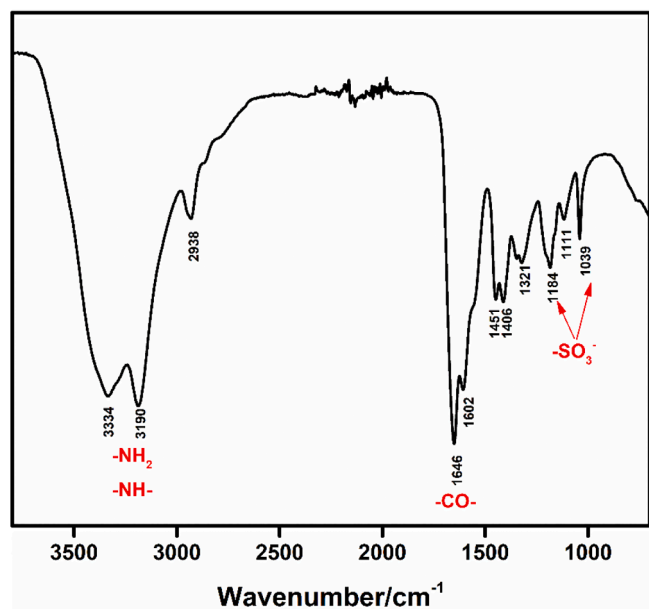
Fig. 5. FT-IR spectrum of CO$_2$-BRPPG, crosslinked copolymer of AM and AMPS.

network. Meanwhile, the polymer chains change from an un-strained state to an elongated configuration. Eventually, a state of equilibrium swelling is achieved in which the net force applied to the polymer network is zero. In addition, high salinity could delay the swelling rate and reduce the equilibrium swelling ratio. The polymer chains in high salinity solutions were highly compressed, and the electric repulsion between polymer chains was also hindered [41,42]. Fig. 6 (b) shows the effect of temperature on the swelling rate and equilibrium swelling ratios. The swelling rate gradually increases with temperature and the equilibrium swelling ratio increases from 34 to 38.5 as the temperature increases from 23 to 45 °C.

The effect of solution pH on the equilibrium swelling ratio was also studied as shown in Fig. 7. Again, 1% NaCl solution was used, and the pH was adjusted by adding dilute HCl or NaOH solution. Fig. 5 demonstrates that solution pH does not significantly affect the equilibrium swelling ratio.

3.3. Self-healing behavior evaluation

The effect of salinity and swelling ratio on the self-healing time was evaluated in this section. As indicated in Fig. 8 (a), the starting time

decreased as the swelling ratio and salinity increased. However, the ending time decreased with the increase of the swelling ratio. For example, in 1% of NaCl solution, the gel particles began to self-heal after 2.5 h with a swelling ratio of 10, and the gel strength became constant after curing at room temperature for four days. However, the ending time decreased to two days when the swelling ratio increased to 30. It should also be mentioned that high salinity can delay the swelling process and hinder the self-healing speed because of the charge screening effect [43]. High salinity, especially the divalent cations, can compress the polymer chains and reduce the reactivity of the carboxylate groups by generating sodium/calcium carboxylate [42,44,45]. In addition, the diffusion rate of the secondary crosslinker/reassembling agent in the high salinity solutions was also hindered because of the less stretched polymer network structure and charge screening effect. Fig. 8 (b) shows the self-healing behavior at different temperatures. The self-healing time gradually decreased as the increase of temperature. The self-healing starting time decreased from 3 h to 80 mins as the temperature increased from 23 to 45 °C.

A fracture model was deployed to study the extrusion and self-healing behaviors of the CO$_2$-BRPPG. As shown in Fig. 9, the CO$_2$-BRPPG began to be produced from the fractures at 20 psi, and the extrudate formed a thick gel cake at 40 psi. After extruding through the fractures, the normal stresses perpendicular to the flow direction are
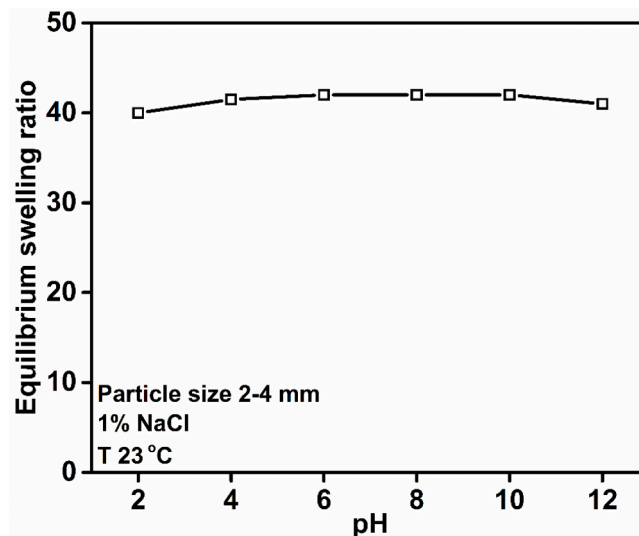

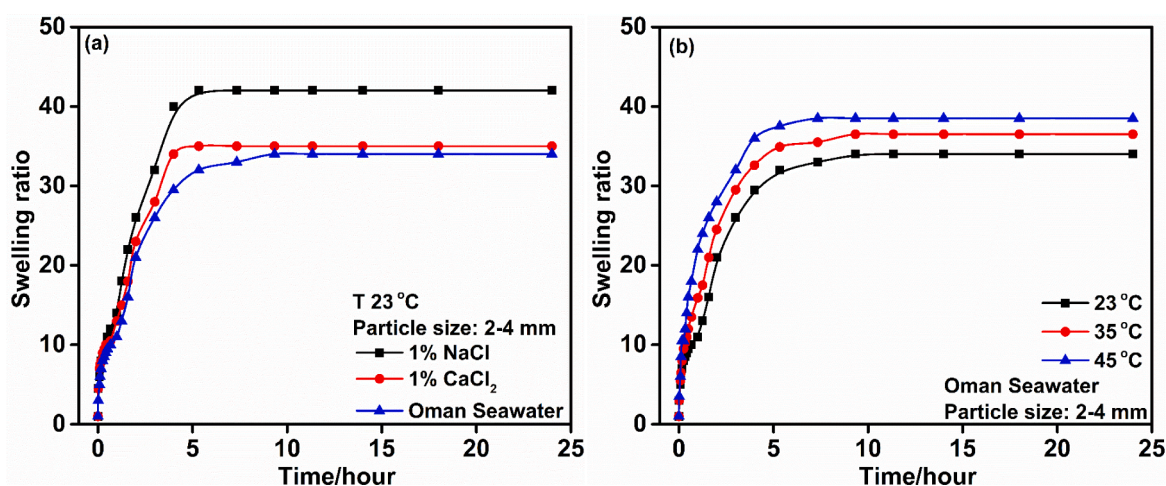**Fig. 7.** Effect of pH on the equilibrium swelling ratio.

Fig. 6. Dynamic swelling kinetics of CO$_2$-BRPPG in different (a) brine solutions, (b) temperatures.
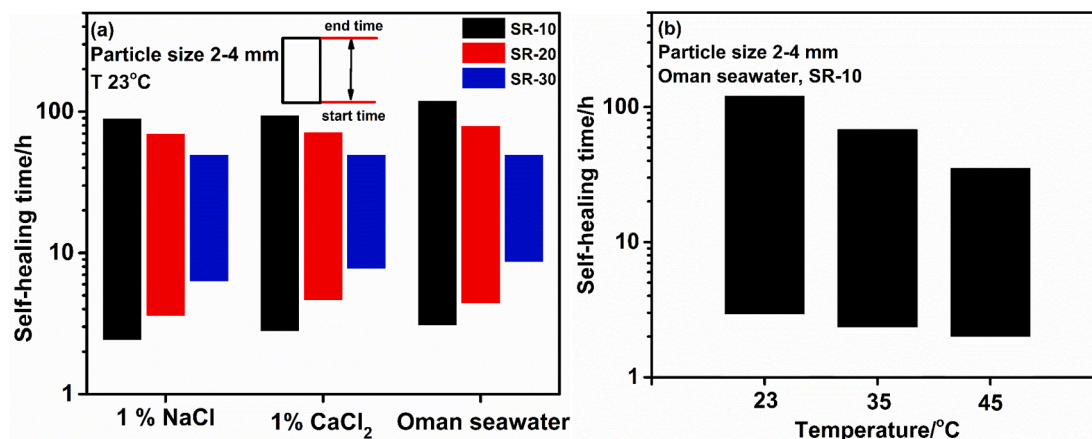
Fig. 8. Effect of (a) salinity and swelling ratio (b) temperature on the self-healing time.
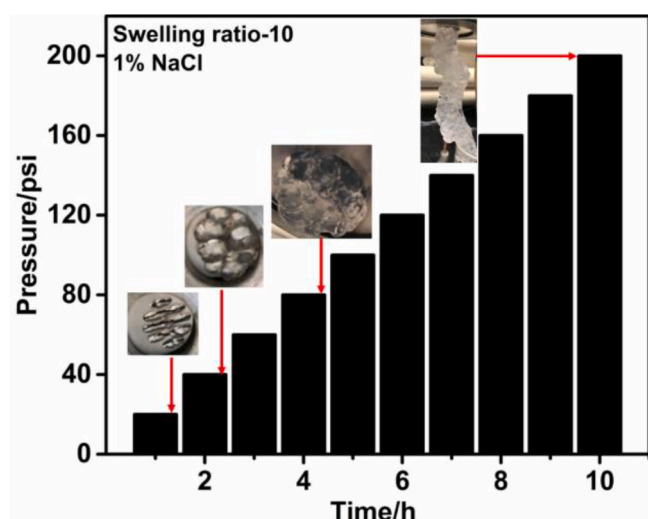

Fig. 9. Self-healing phenomena of the CO_2-BRPPG.

Fig. 10. Elastic modulus of the CO_2-BRPPG.

relieved, and the extrudate begins to swell and expand. Therefore, the strip-shaped gels formed at the beginning gradually transformed into disc-shaped gels. The boundary between the extrudates disappeared, and a uniform bulky gel was re-formed after curing at room temperature for 20 h. In addition, no dehydration was observed during the test.

3.4. Gel strength responding to salinity and swelling ratio

Factors affecting gel strength were studied in this section. Elastic modulus was deployed to evaluate the gel strength. All tests were performed in linear viscoelastic regions, as shown in Fig. 10. The gel strength gradually decreases with the increase of the swelling ratio. For example, the CO_2-BRPPG with a swelling ratio of 3 forms a solid rubber-like bulk gel after self-healing, which also has potential application in wellbore leakage control. Fig. 11 shows the effect of salinity and temperatures on the gel strength. The salinity has a negative impact on the gel strength. For example, the gel strength in 1% NaCl, $CaCl_2$ and Oman seawater at 23 °C were 2194, 1951 and 1865 Pa, respectively. It should be noted that the gel strength increases precipitously with temperature. The elastic modulus at 65 °C increased to 2776 Pa, which is 1.27 times stronger than the gel at 23 °C for the sample prepared in 1% NaCl with a swelling ratio of 10.
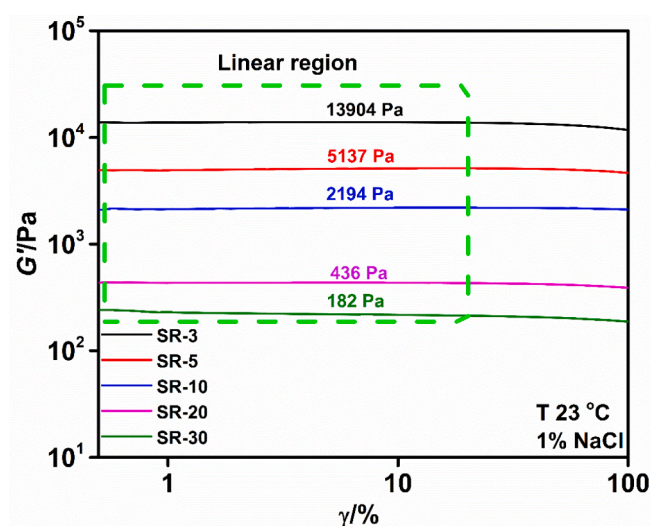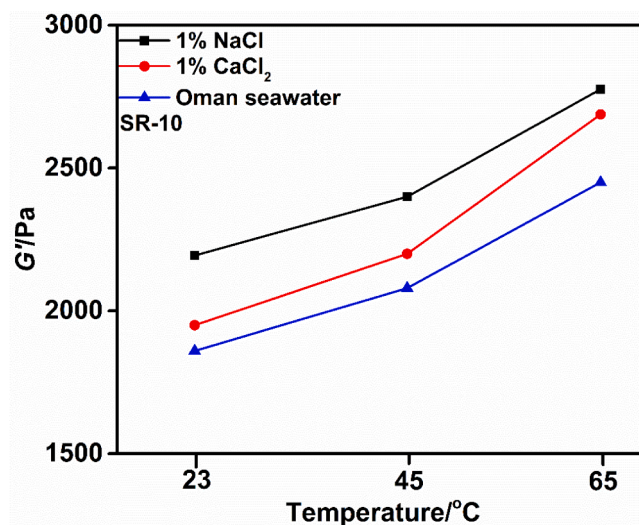

Fig. 11. G' as a function of salinity and temperature.

3.5. CO₂ and thermal stability evaluations

The thermal stability of CO_2-BRPPG has been evaluated at 65 °C in 1% NaCl for more than 200 days with variable swelling ratios. As shown in Fig. 12, the CO_2-BRPPG with swelling ratios of 10, 20 and 30 remained stable so far after being aged for more than 200 days. The fully swelled gel becomes partially flowable after 200 days of aging. However, it is noteworthy that no syneresis/dehydration was observed during the aging test.

Fig. 13 shows the CO_2 stability test results. The testing temperature was 65 °C, and the testing pressure was 750, 1300, and 2900 psi. The gel strength gradually increases with the extension of CO_2 exposure time and the increase of CO_2 pressure. For example, the gel strength increased by almost 20% after 60 days of aging under 2900 psi. The polymer gels expanded and changed to a porous foam gel during the degassing process, as depicted in Fig. 14. When the gels were removed from vessels, we checked whether there existed water in the vessels due to gel dehydration, and we did not observe any water left in the vessel. However, there is a tiny increase in the gel strength after exposure. One possible reason is that during the degassing process, the highly compressed dissolved CO_2 expands and flows out from the gel phase and generates a lot of tiny bubbles in-situ, resulting in an extremely porous structure. Therefore, the dense porous network further enhances the elasticity and strength of the polymer gels.

We also characterized the microstructure of the self-healed CO_2-BRPPG before and after CO_2 exposure. Fig. 15 shows the gel network structure after 60 days of exposure to 2900 psi CO_2 at 65 °C. The polymer gel network structure collapsed slightly after exposure, but it still maintained its network integrity. This also confirmed that the CO_2-BRPPG was stable in supercritical CO_2 conditions.

3.6. Supercritical CO₂ plugging test

The plugging performance was mainly controlled by two factors: the mechanical strength of the gel plugs and the adhesion strength between the gel plugs and rocks. A fractured sandstone model was deployed to evaluate the plugging performance of the CO_2-BRPPG.

Fig. 16 shows the core-flooding test of the CO_2-BRPPG. The supercritical CO_2 breakthrough pressure was 265 psi/feet (5.48 MPa/m). After the supercritical CO_2 breakthrough, as the injection rate increased from 1 to 100 feet/day, the *Frr* decreased from 10^7 to 10^5, and the
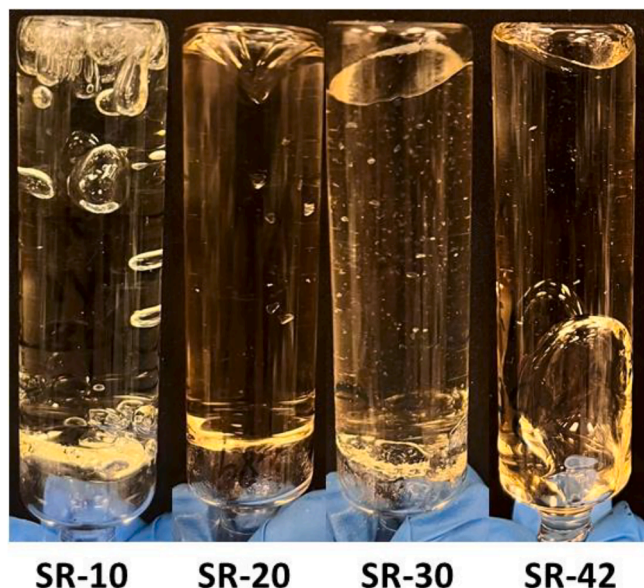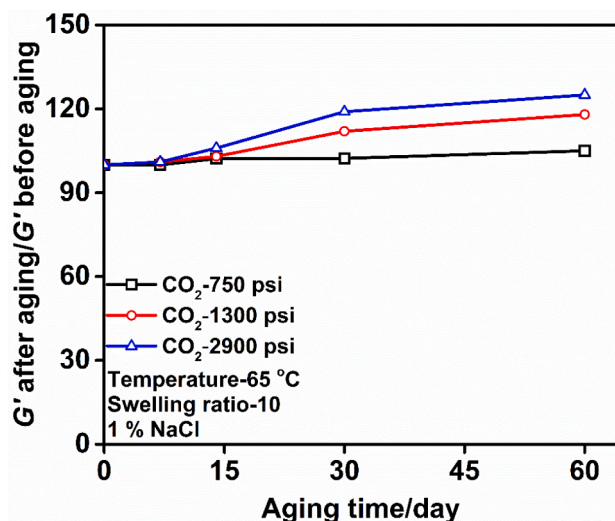
Fig. 13. Gel strength changes during the CO_2 stability tests.

plugging efficiency reached over 99.99%. As shown in Fig. 16 c, we can still find a large amount of sticky gel remaining on the fracture surface even after the supercritical CO_2 breakthrough and *Frr* tests. In contrast, the breakthrough pressures of the conventional PPG are usually less than 50 psi/feet (1.03 MPa/m), and large amounts of gel particles were pushed out from the fracture after the water breakthrough [46]. This is because PPG lacks particle–particle association and particle rock adhesion. There is no strong physical or chemical interaction between different gel particles that could enhance the particle association.

According to coating chemistry, the adhesion strength between polymers and rocks increased with the increase of the flexibility and polarity of the polymer gels [47,48]. For this novel CO_2-BRPPG, the primary network built by the MBA is loose. Thus, it is much easier for the CO_2-BRPPG to penetrate into the micro-pores of the rock surface with the external pressure, and the adhesion was further enhanced by mechanical interlocking, as shown in Fig. 17 [48]. Besides, the polarity of the CO_2-BRPPG was greatly enhanced by adding the ionic re-assembling agent. Thus the polymer gels can better interact with the polar groups on the rock surface, such as hydroxyl groups. Therefore, the polymer gel and rock adhesion behavior are greatly enhanced.

3.7. Tensile and adhesion tests

Most publications only emphasized the importance of mechanical strength in the fracture plugging treatment, but the adhesion behavior of the gels should be treated equally. This is because the adhesive force is another crucial factor determining the residual volume of polymer gels in the fracture after the water or gas breakthrough.

Therefore, to better explain the core flooding result, we studied the tensile and adhesion behavior of this CO_2-BRPPG. Fig. 18 shows the tensile behavior of the CO_2-BRPPG. The maximum load pressures of CO_2-BRPPG with swelling ratios 3, 5, 10 and 20 were 4.7, 2.8, 1.3 and 0.5 N, respectively. Besides, the CO_2-BRPPG with a swelling ratio of 10 did not break during the test. Therefore, we demonstrated that the CO_2-BRPPG has excellent mechanical strength and elasticity through gel strength and tensile tests.

The adhesion strength of the CO_2-BRPPG was evaluated by measuring the detaching strength. Gels with swelling ratios of 10, 20, and 30 were used for the adhesion strength test. As depicted in Fig. 19, the adhesion strength decreased with the increase of the swelling ratio. In the case of sandstone, the adhesion strength gradually reduced from 1.156 to 0.289 psi as the swelling ratio increased from 10 to 30. This is because the polymer concentration decreases with the increase in the swelling ratio. The increased swelling ratio caused a dilution of the
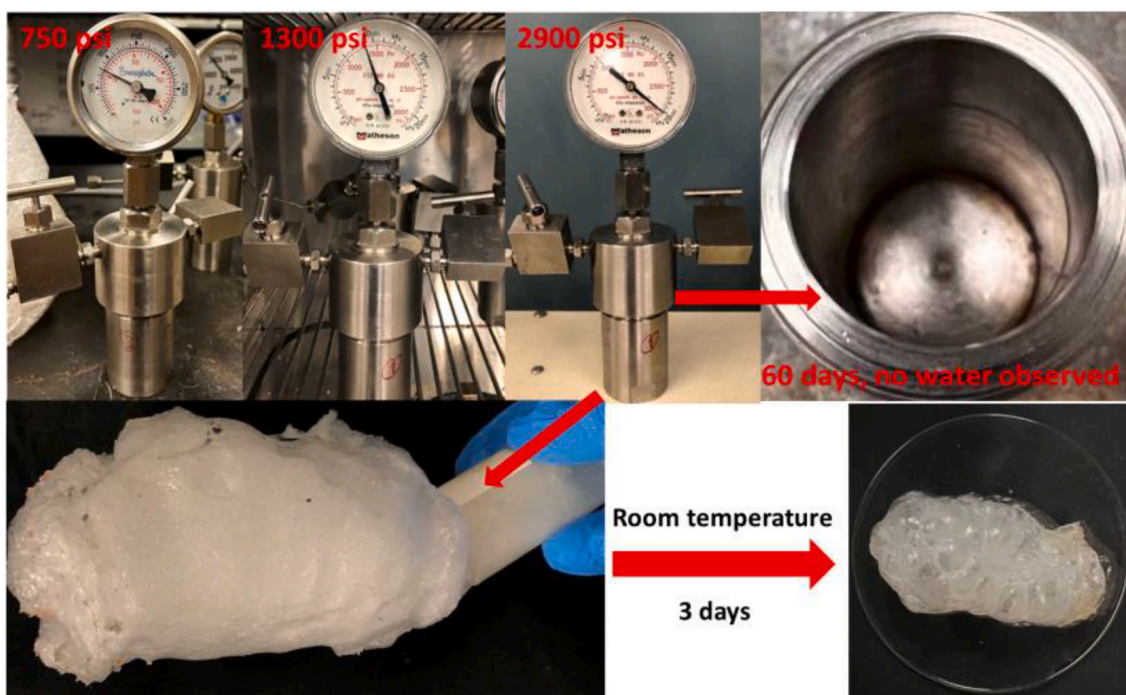
Fig. 12. Gel appearance after 200 days of aging at 65 °C.

Fig. 14. High pressure-resistant stainless-steel vessels and gel appearance after long-term CO_2 exposure.
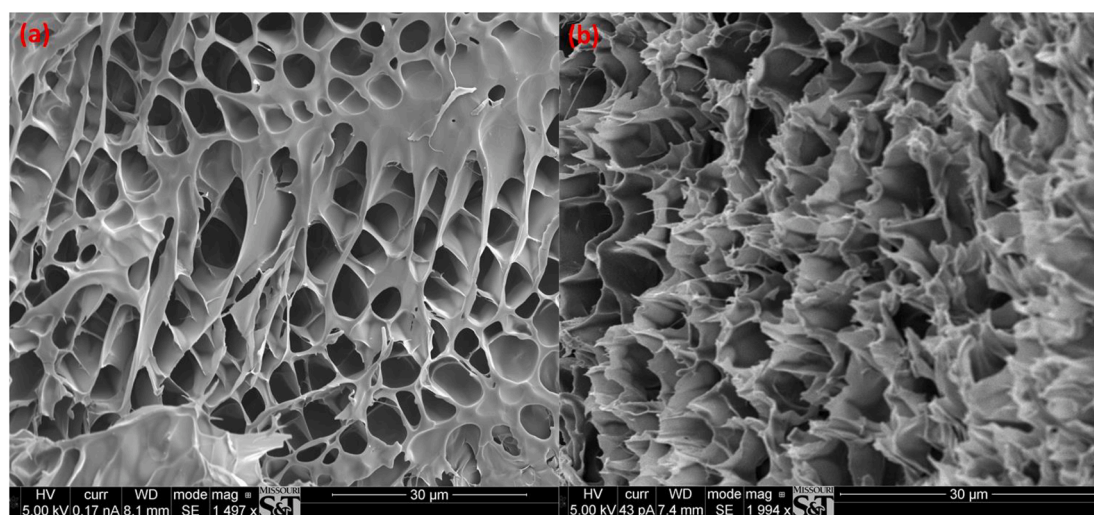

Fig. 15. The microstructure of the CO_2-BRPPG (a) before, (b) after two months of exposure to 2900 psi CO_2.

entanglement structure, excessively lowering the modulus and making the material too fluid-like, leading to a decrease in adhesion [49]. In addition, the CO_2-BRPPG has better adhesion behavior to sandstone over carbonate. This is because the sandstone is mainly composed of quartz, and the surface is usually negatively charged with abundant -Si-OH groups which facilitate the association between positively charged Zr (IV), and $-NH_3^+$ [50]. However, the carbonate rocks are composed of a full Ca/Mg chemical gradient from limestone to dolomite, and the carbonate rock is usually positively charged because of the adsorbed Ca/Mg ions on the rock surface [51–53]. Furthermore, the adsorbed Ca/Mg ions on the rock surface could compete with Zr (IV), and $-NH_3^+$ for the hydroxyl groups, which impairs the association strength between polymer gels and rock surfaces. Therefore, the polymer gels have better adhesion behavior to sandstone over carbonate. CO_2-BRPPG with a swelling ratio of 10 has the highest adhesion strength, which is around four times higher than the gel with a swelling ratio of 30. The results demonstrated

that this novel CO_2-BRPPG has excellent adhesion to rocks, proving the plugging mechanism mentioned above.

3.8. Further discussion

In the case of rock matrix treatment, in-situ gel systems are often used to alleviate reservoir heterogeneity. In-situ gel treatment involves injecting low concentration polymer (0.1 ~ 3 wt%) solution and cross-linker solution, and the hybrid solution could change to gels under reservoir conditions. Under the scenario of no CO_2 breaking through the gel phase, the crosslinked polymer gels have good CO_2 plugging efficiency and long-term stability because of limited contacting areas with supercritical CO_2 [20,54]. However, after the CO_2 breakthrough, the plugging efficiency decreased dramatically, and severe degradation and syneresis can be observed. This is because, after the CO_2 breakthrough, one or several channels were created in the gel phase, which resulted in
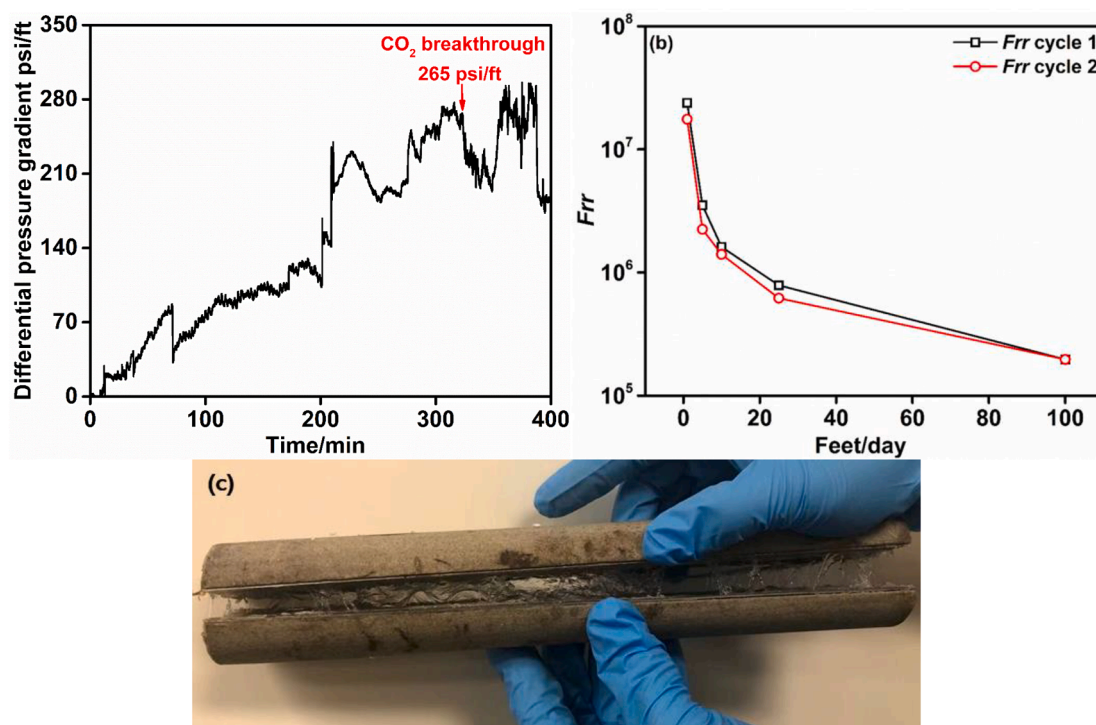
Fig. 16. Fractured core flooding test (a) injection and breakthrough test, (b) *Frr* as a function of injection rate, (c) Fracture surfaces after flooding test.
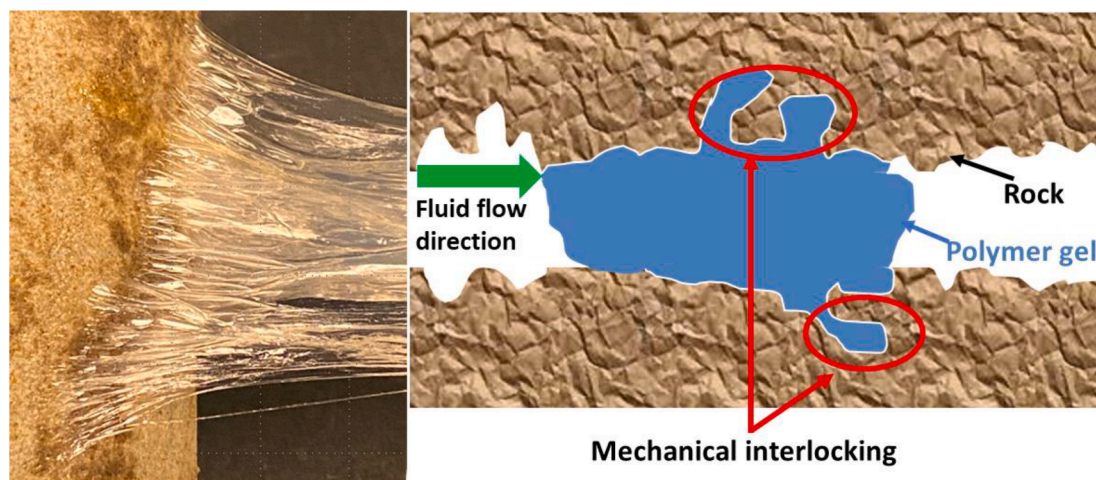

Fig. 17. The adhesion property of the CO_2-BRPPG.

the increased contacting area between the polymer gels and CO_2. Therefore, chain degradation and hydrolysis are significantly accelerated under this scenario [55,56] In the case of fracture or void space conduits treatment, where polymer gels have more contact area with CO_2, most gel systems can not provide good CO_2 plugging efficiency and long-term stability. Moreover, for the in-situ polymer gels, the polymer gel can not provide enough resistance to the high-pressure CO_2 due to the weak gel strength [54]. In addition, conventional PPG products suffer severe hydrolysis under supercritical CO_2 conditions. Field treatment in Cowden Unit in Texas showed that the PPG could plug a high permeability thief zone initially, but the treatment was only effective for five months [24]. Our group has already done some work evaluating the CO_2 stability of PPG products. For example, the cross-linked poly(acrylamide-co-acylate) based PPG is not stable under supercritical CO_2 conditions, and the dehydration ratio ranges from 7 to 55% depending on the salinity and exposure duration [31]. On the other

hand, the CO_2 stability of PPG can be improved by introducing CO_2-resistant monomers such as 2-acrylamido-2-methylpropanesulfonic acid and Sodium 4-vinylbenzenesulfonate [25]. The PPG with CO_2-resistant monomers has excellent supercritical CO_2 stability, and the swelling ratio and elastic modulus remained constant during the 6-month aging test.

Compared with these gel systems, current CO_2-BRPPG is a unique product with self-healing ability, high mechanical strength and adhesion behavior, which could be a potential candidate for the CO_2 plugging and CO_2 sequestration in reservoirs with fractures and void space conduits.

4. Conclusions

A novel branched self-healable preformed particle gel system was systematically evaluated in this work to see whether it can be used to plug fractures in CO_2 flooding and CO_2 storage reservoirs. The effect of
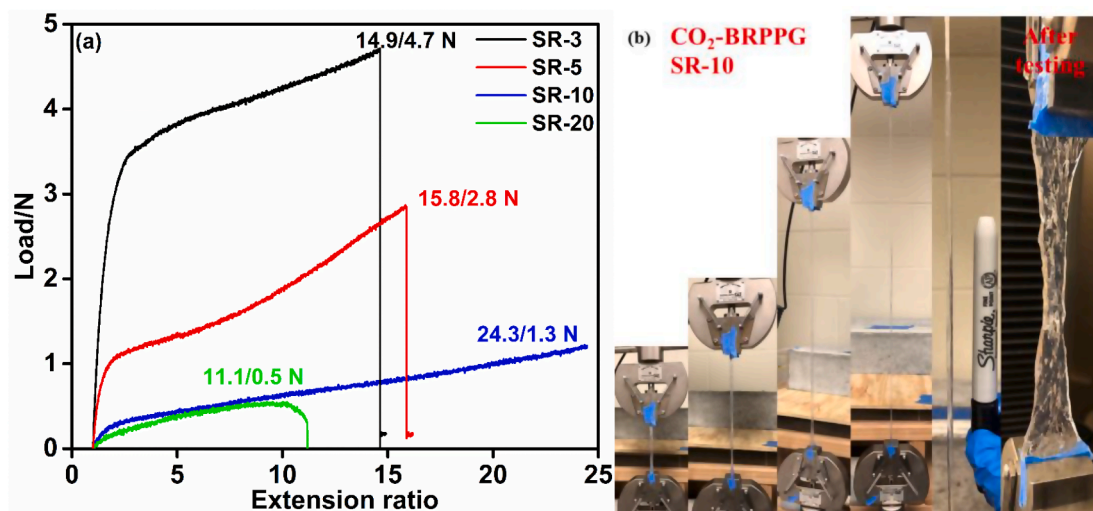
Fig. 18. Tensile test (a) CO_2-BRPPG with different swelling ratios; (d) Gel appearance during the test.
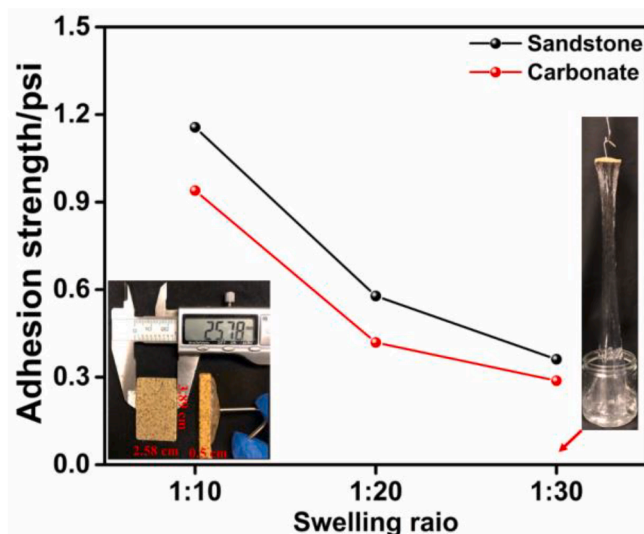

Fig. 19. Adhesion strength as a function of swelling ratio.

pH and salinity on the CO_2-BRPPG swelling behavior was studied. CO_2-BRPPG has an equilibrium swelling ratio of 42 in 1% NaCl solution at room temperature. This novel particle gel can re-form a bulky adhesive gel in different brine solutions, and the bulky gel also has self-healing properties. The self-healed bulk gel has an elastic modulus up to 2194 Pa with a swelling ratio of 10. The self-healed gel has good thermal and phase stability in supercritical CO_2 conditions. No syneresis was observed during the long-term stability tests. In addition, the CO_2-BRPPG has good plugging efficiency in the fractured model, and the core flooding test showed that the supercritical CO_2 breakthrough pressure could reach up to 265 psi/feet (5.48 MPa/m). The tensile and adhesion tests further explained the excellent plugging efficiency. CO_2-BRPPG with a swelling ratio of 10 has a maximum load of 1.3 N, and the adhesion strength reaches 1.16 psi. The superior mechanical, adhesion strength and thermal/phase stability make this CO_2-BRPPG a good candidate as a plugging material for CO_2 storage and CO_2 flooding projects.

Declaration of Competing Interest

The authors declare that they have no known competing financial interests or personal relationships that could have appeared to influence

the work reported in this paper.

Appendix A. Supplementary data

Supplementary data to this article can be found online at https://doi.org/10.1016/j.cej.2022.136635.

References

[1] C.A. Castaneda-Herrera, G.W. Stevens, R.R. Haese, Review of CO_2 leakage mitigation and remediation technologies, Geological Carbon Storage: Subsurface Seals and Caprock Integrity (2018) 327–337, https://doi.org/10.1002/9781119118657.ch16.
[2] S. Iglauer, C. Pentland, A. Busch, CO_2 wettability of seal and reservoir rocks and the implications for carbon geo-sequestration, Water Resour. Res. 51 (2015) 729–774, https://doi.org/10.1002/2014WR015553.
[3] E. Mohagheghian, H. Hassanzadeh, Z. Chen, CO_2 sequestration coupled with enhanced gas recovery in shale gas reservoirs, J. CO2 Util. 34 (2019) 646–655, https://doi.org/10.1016/j.jcou.2019.08.016.
[4] R. Bailey, M. McDonald, CO_2 capture and use for EOR in Western Canada 1. General overview, Energy Convers. Manag. 34 (1993) 1145–1150, https://doi.org/10.1016/0196-8904(93)90063-G.
[5] J. Zhou, J. Zhang, J. Yang, Z. Jin, K.H. Luo, Mechanisms for kerogen wettability transition from water-wet to CO_2-wet: Implications for CO_2 sequestration, Chem. Eng. J. 428 (2022), 132020, https://doi.org/10.1016/j.cej.2021.132020.
[6] Y. Liu, Z. Rui, A storage-driven CO_2 EOR for a net-zero emission target, Engineering. (2022), https://doi.org/10.1016/j.eng.2022.02.010.
[7] Y. Liu, Z. Rui, T. Yang, B. Dindoruk, Using propanol as an additive to CO_2 for improving CO_2 utilization and storage in oil reservoirs, Appl. Energy. 311 (2022), 118640.
[8] G. Cui, Y. Wang, Z. Rui, B. Chen, S. Ren, L. Zhang, Assessing the combined influence of fluid-rock interactions on reservoir properties and injectivity during CO_2 storage in saline aquifers, Energy. 155 (2018) 281–296.
[9] G. Cui, S. Ren, Z. Rui, J. Ezekiel, L. Zhang, H. Wang, The influence of complicated fluid-rock interactions on the geothermal exploitation in the CO_2 plume geothermal system, Appl. Energy. 227 (2018) 49–63.
[10] F. Gozalpour, S.R. Ren, B. Tohidi, CO_2 EOR and storage in oil reservoir, Oil Gas Sci. Technol. 60 (2005) 537–546, https://doi.org/10.2516/ogst:2005036.
[11] F. Orr Jr, J. Taber, Use of carbon dioxide in enhanced oil recovery, Science. 224 (1984) 563–569, https://doi.org/10.1126/science.224.4649.563.
[12] K.S. Lackner, A guide to CO_2 sequestration, Science. 300 (2003) 1677–1678, https://doi.org/10.1126/science.1079033.
[13] A.-C. Aycaguer, M. Lev-On, A.M. Winer, Reducing carbon dioxide emissions with enhanced oil recovery projects: A life cycle assessment approach, Energy Fuels. 15 (2001) 303–308, https://doi.org/10.1021/ef000258a.
[14] D.L. Bishop, M.E. Williams, S.E. Gardner, D.P. Smith, T.D. Cochrane, Vertical conformance in a mature carbonate CO_2 flood: Salt Creek Field Unit, Texas, Abu

Dhabi International Conference and Exhibition (2004), https://doi.org/10.2118/88720-MS.

[15] R. Seright, Reduction of gas and water permeabilities using gels, SPE Prod. Oper. 10 (1995) 103–108, https://doi.org/10.2118/25855-PA.

[16] R.D. Sydansk, A new conformance-improvement-treatment chromium(III) gel technology, SPE Enhanced Oil Recovery Symposium (1988), https://doi.org/10.2118/17329-MS.

[17] S. Vossoughi, Profile modification using in situ gelation technology-a review, J. Pet. Sci. Eng. 26 (2000) 199–209, https://doi.org/10.1016/S0920-4105(00)00034-6.

[18] K.L.N.P. de Aguiar, P.F. de Oliveira, C.R.E. Mansur, A comprehensive review of in situ polymer hydrogels for conformance control of oil reservoirs, Oil Gas Sci. Technol.-Rev. IFP Energies nouvelles. 75 (2020) 8, https://doi.org/10.2516/ogst/2019067.

[19] F. Martin, F. Kovarik, Chemical gels for diverting CO2: Baseline experiments, SPE annual technical conference and exhibition (1987), https://doi.org/10.2118/16728-MS.

[20] L. Taabbodi, K. Asghari, Application of in-depth gel placement for water and carbon dioxide conformance control in carbonate porous media, J. Can. Pet. Technol. 45 (2006), https://doi.org/10.2118/06-02-02.

[21] R. Seright, Use of preformed gels for conformance control in fractured systems, SPE Prod. Oper. 12 (1997) 59–65, https://doi.org/10.2118/35351-PA.

[22] J.-P. Coste, Y. Liu, B. Bai, In-depth fluid diversion by pre-gelled particles. laboratory study and pilot testing, SPE/DOE improved oil recovery symposium, 2000. https://doi.org/10.2118/59362-MS.

[23] R.S. Seright, J. Liang, A comparison of different types of blocking agents, SPE European Formation Damage Conference (1995), https://doi.org/10.2118/30120-ms.

[24] C. Green, P. Creel, S. McDonald, T. Ryan, Utilization of a crystallized hydrating copolymer to modify an injectivity problem in a horizontal CO2 WAG injector in the South Cowden Unit, Ector County, Texas—Post treatment coil tubing acidizing stimulation—Case history, Southwestern Petroleum Short Course, Lubbock, TX, 2003.

[25] Z. Wang, B. Bai, Y. Long, L. Wang, An investigation of CO2-responsive preformed particle gel for conformance control of CO2 flooding in reservoirs with fractures or fracture-like channels, SPE J. 24 (2019) 2398–2408, https://doi.org/10.2118/197046-PA.

[26] G. Targac, C. Gallo, D. Smith, C.-K. Huang, S. Autry, J. Peirce, L. Baohong, Case history of conformance solutions for west sak wormhole/void space conduit with a new reassembling pre-formed particle gel RPPG, SPE Annual Technical Conference and Exhibition (2020), https://doi.org/10.2118/201302-MS.

[27] D.D. Smith, M.J. Giraud, C. Kemp, M.S. McBee, J. Taitano, M. Winfield, J. Portwood, D.M. Everett, The succesful evolution of Anton Irish conformance efforts, SPE annual technical conference and exhibition (2006), https://doi.org/10.2118/103044-MS.

[28] Z. Wang, B. Bai, Preformed-particle-gel placement and plugging performance in fractures with tips, SPE J. 23 (2018) 2316–2326, https://doi.org/10.2118/193997-PA.

[29] L. Wang, Y. Long, H. Ding, J. Geng, B. Bai, Mechanically robust re-crosslinkable polymeric hydrogels for water management of void space conduits containing reservoirs, Chem. Eng. J. 317 (2017) 952–960, https://doi.org/10.1016/j.cej.2017.02.140.

[30] X. Sun, Y. Long, B. Bai, M. Wei, S. Suresh, Evaluation and plugging performance of carbon dioxide-resistant particle gels for conformance control, SPE J. 25 (2020) 1745–1760, https://doi.org/10.2118/200493-PA.

[31] X. Sun, S. Suresh, X. Zhao, B. Bai, Effect of supercritical CO2 on the dehydration of polyacrylamide-based super-absorbent polymer used for water management, Fuel. 224 (2018) 628–636, https://doi.org/10.1016/j.fuel.2018.03.103.

[32] F.D. Tovar, M.A. Barrufet, D.S. Schechter, Long term stability of acrylamide based polymers during chemically assisted CO2 WAG EOR, SPE improved oil recovery symposium, OnePetro (2014), https://doi.org/10.2118/169053-MS.

[33] P. Woods, K. Schramko, D. Turner, D. Dalrymple, E. Vinson, In-situ polymerization controls CO2/water channeling at Lick Creek, SPE enhanced oil recovery symposium, OnePetro (1986), https://doi.org/10.2118/14958-MS.

[34] J. Pu, B. Bai, A. Alhuraishawy, T. Schuman, Y. Chen, X. Sun, A recrosslinkable preformed particle gel for conformance control in heterogeneous reservoirs

containing linear-flow features, SPE J. 24 (2019) 1714–1725, https://doi.org/10.2118/191697-PA.

[35] F.D. Tovar, M.A. Barrufet, D.S. Schechter, Long term stability of acrylamide based polymers during chemically assisted CO2 WAG EOR, SPE Improved Oil Recovery Symposium (2014), https://doi.org/10.2118/169053-MS.

[36] M.W. Conway, S.W. Almond, J.E. Briscoe, L.E. Harris, Chemical model for the rheological behavior of crosslinked fluid systems, J. Pet. Technol. 35 (1983) 315–320, https://doi.org/10.2118/9334-PA.

[37] Z. Wei, J.H. Yang, J. Zhou, F. Xu, M. Zrínyi, P.H. Dussault, Y. Osada, Y.M. Chen, Self-healing gels based on constitutional dynamic chemistry and their potential applications, Chem. Soc. Rev. 43 (2014) 8114–8131, https://doi.org/10.1039/C4CS00219A.

[38] H. Jiang, G. Zhang, X. Feng, H. Liu, F. Li, M. Wang, H. Li, Room-temperature self-healing tough nanocomposite hydrogel crosslinked by zirconium hydroxide nanoparticles, Compos Sci Technol. 140 (2017) 54–62, https://doi.org/10.1016/j.compscitech.2016.12.027.

[39] S. Hou, P.X. Ma, Stimuli-responsive supramolecular hydrogels with high extensibility and fast self-healing via precoordinated mussel-inspired chemistry, Chem. Mater. 27 (2015) 7627–7635, https://doi.org/10.1021/acs.chemmater.5b02839.

[40] P.J. Flory, Principles of polymer chemistry, 1953.

[41] T. Tanaka, D.J. Fillmore, Kinetics of swelling of gels, Chem. Phys. 70 (1979) 1214–1218, https://doi.org/10.1063/1.437602.

[42] T. Tanaka, Gels, SciAm. 244 (1981) 124-S-117. https://www.jstor.org/stable/24964265.

[43] S. Sircar, J.P. Keener, A.L. Fogelson, The effect of divalent vs. monovalent ions on the swelling of Mucin-like polyelectrolyte gels: Governing equations and equilibrium analysis, Chem. Phys. 138 (1) (2013) 014901.

[44] P. DiGiacomo, Mechanism of polyacrylamide gel syneresis determined by C-13 NMR, SPE Oilfield and Geothermal Chemistry Symposium (1983), https://doi.org/10.2118/11787-MS.

[45] R.D. Sydansk, Acrylamide-polymer/chromium (III)-carboxylate gels for near wellbore matrix treatments, SPE Advanced Technology Series. 1 (1993) 146–152, https://doi.org/10.2118/20214-PA.

[46] A. Imqam, B. Bai, Optimizing the strength and size of preformed particle gels for better conformance control treatment, Fuel. 148 (2015) 178–185.

[47] C.M. Miller, Adhesion and the surface energy components of natural minerals and aggregates, Texas A & M University, 2011.

[48] F.N. Jones, M.E. Nichols, S.P. Pappas, Organic coatings: science and technology (2017).

[49] M. Dompé, M. Vahdati, F. van Ligten, F.J. Cedano-Serrano, D. Hourdet, C. Creton, M. Zanetti, P. Bracco, J. van der Gucht, T. Kodger, M. Kamperman, Enhancement of the adhesive properties by optimizing the water content in PNIPAM-functionalized complex coacervates, ACS Appl. Polym. Mater. 2 (4) (2020) 1722–1730.

[50] J.H. Waite, Mussel adhesion–essential footwork, J. Exp. Biol. 220 (2017) 517–530, https://doi.org/10.1242/jeb.134056.

[51] Y. Daoxian, 6.26 Variations of Karst Geomorphology over Geoclimatic Gradients, (2013). https://doi.org/10.1016/B978-0-12-374739-6.00107-X.

[52] B.J. Chun, S.G. Lee, J.I. Choi, S.S. Jang, Adsorption of carboxylate on calcium carbonate (101 4) surface: Molecular simulation approach, Colloids Surf. A: Physicochem. Eng. Asp. 474 (2015) 9–17, https://doi.org/10.1016/j.colsurfa.2015.03.003.

[53] R. Khaledialidusti, J. Kleppe, Surface-charge alteration at the carbonate/brine interface during single-well chemical-tracer tests: Surface-complexation model, SPE J. 23 (2018) 2302–2315, https://doi.org/10.2118/191356-PA.

[54] A.H. Al-Ali, D.S. Schechter, R.H. Lane, Application of polymer gels as conformance control agents for carbon dioxide EOR WAG floods, SPE International Symposium on Oilfield Chemistry (2013), https://doi.org/10.2118/164096-MS.

[55] X. Sun, B. Bai, Y. Long, Z. Wang, A comprehensive review of hydrogel performance under CO2 conditions for conformance control, J. Pet. Sci. Eng. 185 (2020), 106662, https://doi.org/10.1016/j.petrol.2019.106662.

[56] X. Sun, B. Bai, A.K. Alhuraishawy, D. Zhu, Understanding the plugging performance of HPAM-Cr (III) polymer gel for CO2 conformance control, SPE J. 26 (2021) 3109–3118, https://doi.org/10.2118/204229-PA.